ACS Catalysis

Research Article

pubs.acs.org/acscatalysis

Base-Free Methanol Dehydrogenation Using a Pincer-Supported Iron Compound and Lewis Acid Co-catalyst

Elizabeth A. Bielinski,[†] Moritz Förster,[‡] Yuanyuan Zhang,[§] Wesley H. Bernskoetter,*[,§] Nilay Hazari,*[,†] and Max C. Holthausen*[,‡]

[†]Department of Chemistry, Yale University, P.O. Box 208107, New Haven, Connecticut 06520, United States

[‡]Institut für Anorganische und Analytische Chemie, Goethe-Universität, Max-von-Laue-Strasse 7, 60438 Frankfurt am Main, Germany

[§]Department of Chemistry, Brown University, Providence, Rhode Island 02912, United States

Supporting Information

ABSTRACT: Hydrogen is an attractive alternative energy vector to fossil fuels if effective methods for its storage and release can be developed. In particular, methanol, with a gravimetric hydrogen content of 12.6%, is a promising target for chemical hydrogen storage. To date, there are relatively few homogeneous transition metal compounds that catalyze the aqueous phase dehydrogenation of methanol to release hydrogen and carbon dioxide. In general, these catalysts utilize expensive precious metals and require a strong base. This paper shows that a pincer-supported Fe compound and a co-catalytic amount of a Lewis acid are capable of catalyzing base-free aqueous phase methanol dehydrogenation with turnover numbers up to 51 000. This is the highest turnover number reported for either a first-row transition metal or a base-free system. Additionally, this paper describes preliminary mechanistic experiments to understand the reaction pathway and propose a stepwise process, which requires metal−ligand cooperativity. This pathway is supported by DFT calculations and explains the role of the Lewis acid co-catalyst.

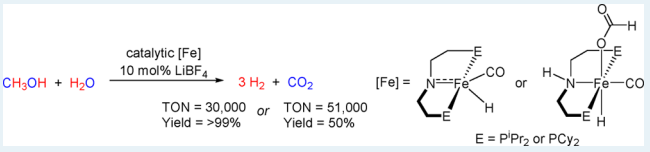

KEYWORDS: *iron, catalysis, methanol dehydrogenation, metal−ligand cooperativity, pincer ligands, DFT calculations*

INTRODUCTION

As the worldwide demand for energy increases, the development of large-scale alternatives to fossil fuels will become more important from both environmental and economic standpoints.[1] H_2 is a potential clean energy source as its combustion results only in the generation of water as a byproduct.[2] In particular, chemical H_2 storage (CHS) based on the reversible (de)hydrogenation of organic molecules represents a method by which a liquid organic carrier (LOC) may serve as a safe and easily transportable fuel.[3] The selective release of H_2 from a LOC, followed by either direct combustion or use as a feedstock in a proton-exchange membrane fuel cell,[4] would allow for the generation of energy from H_2 while avoiding the dangers and difficulties associated with its transport.[3] Methanol (MeOH) is a promising target for CHS,[3a,5] as it has a high gravimetric H_2 content (12.6%) and can be dehydrogenated in the presence of water to release 3 equiv of H_2 (eq 1). Furthermore, it can be generated from renewable sources.[5b]

$$CH_3OH + H_2O \rightarrow 3H_2 + CO_2 \quad (1)$$

Currently in re-formed MeOH fuel cells, heterogeneous catalysts are used to release H_2 from MeOH for the generation of electricity.[3a,6] These catalysts operate at high temperatures and pressures and produce a significant amount of CO, which ultimately poisons the fuel cell.[3a,6a] Although there has been ongoing research into the development of homogeneous catalysts for MeOH dehydrogenation since the 1980s,[7] only recently have a number of well-defined systems that can catalyze the full dehydrogenation of MeOH and water to H_2 and CO_2 been reported (Table 1).[8] These systems generally operate at significantly lower temperatures than heterogeneous catalysts and produce less CO. However, to date the most active homogeneous catalysts are based on expensive precious metals such as Ru,[8b] and with the exception of Grützmacher's seminal system,[8a] require either the use of a strong base or a precious metal co-catalyst.

The only reported first-row transition metal catalyst for MeOH dehydrogenation was described by Beller and co-workers.[8c] This complex, ($^{iPr}PN^{H}P$)Fe(CO)H(HBH_3) (^{iPr}PNP = N($CH_2CH_2P^iPr_2$)$_2$, **C**),[9] features a bifunctional PNP ligand and is able to achieve ∼10 000 TONs in the presence of 8 M KOH. We, along with several other groups, have been studying the related amido compounds (^{R}PNP)FeH(CO) (^{R}PNP = N{$CH_2CH_2(PR_2)$}$_2$; R = ^{i}Pr (**1a**) or Cy (**1b**)),[10] which in the case of **1a** can be formed by the addition of base to **C**. It has been demonstrated that **1a** can dehydrogenate primary alcohols such as 1-butanol to the corresponding esters without a base or H_2 acceptor (Scheme 1),[10e] whereas **1a** and **1b** can be used as

Received: January 22, 2015
Revised: March 3, 2015
Published: March 5, 2015

DOI: 10.1021/acscatal.5b00137
ACS Catal. 2015, 5, 2404−2415

Table 1. Homogeneous Transition Metal Catalysts for Aqueous Phase MeOH Dehydrogenation to CO_2 and H_2

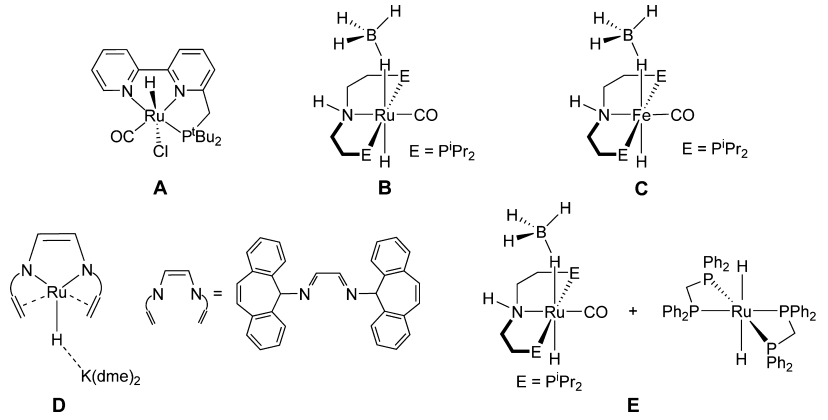

catalyst	ratio MeOH/H_2O	solvent	additive	TON	yield (%)	reference
A	1:1 MeOH/H_2O	toluene	KOH	28,000	77	Milstein[8d]
B	4:1 MeOH/H_2O	neat	8 M KOH	350,000	27	Beller[8b]
C	4:1 MeOH/H_2O	neat	8 M KOH	9800	6	Beller[8c]
D	1:1 MeOH/H_2O	THF		540	90	Grützmacher[8a]
E	4:1 MeOH/H_2O	triglyme		4200	26	Beller[8e]

Scheme 1. Summary of Selected Previous and Current Reactions Catalyzed by 1a, 1b, 2a, and 2b

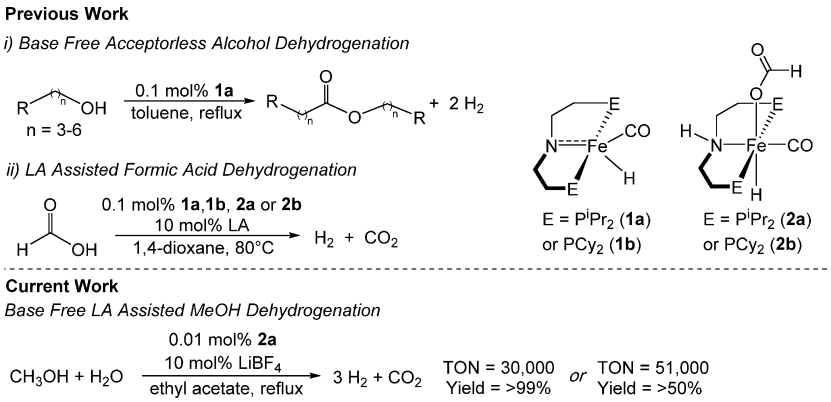

highly efficient catalysts for formic acid dehydrogenation in combination with a Lewis acid (LA).[10d] Similarly, the related formate complexes **2a** and **2b**, which are proposed to generate **1a** and **1b** in situ, are also active catalysts for formic acid dehydrogenation in the presence of a LA.[10d] Herein we demonstrate that **1a**, **1b**, **2a**, and **2b** in the presence of a LA co-catalyst can be used as catalysts for the dehydrogenation of MeOH without added base. We report a maximum TON of ~51 000, the highest for either a first-row transition metal based catalyst or a base free system. In addition, we describe preliminary mechanistic studies and suggest a connection between Beller's catalyst **C** and **1a**.

RESULTS AND DISCUSSION

Previously it has been proposed that the complete aqueous phase dehydrogenation of MeOH to CO_2 and H_2 occurs following the stepwise pathway shown in Scheme 2.[8a,b] Initial dehydrogenation of MeOH produces formaldehyde and releases 1 equiv of H_2. Subsequently, the reaction of water with formaldehyde generates methanediol, which undergoes a second dehydrogenation to produce formic acid and a second equivalent of H_2. Finally, formic acid dehydrogenation results in the release of the third equivalent of H_2, along with CO_2. Given that **1a** and related Fe complexes catalyze both the dehydrogenation of primary alcohols such as 1-butanol to esters (analogous to steps i–iii in Scheme 2) and formic acid dehydrogenation (step iv in Scheme 2) without a base, we postulated that they may be able to perform base-free aqueous phase MeOH dehydrogenation if compatible conditions for both reactions could be developed. To achieve this tandem reaction we pursued a strategy in which we first studied the dehydrogenation of MeOH in the absence of water (step i) and then explored full aqueous phase MeOH dehydrogenation.

Scheme 2. Proposed Stepwise Pathway for Aqueous Phase Dehydrogenation of MeOH to CO_2 and H_2

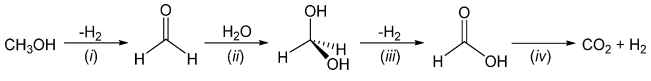

MeOH Dehydrogenation in the Absence of Water. Although catalysts **1a** and **1b** were used to dehydrogenate primary alcohols,[10e] MeOH was not used as a substrate. Initially, we screened conditions for the dehydrogenation of MeOH in the absence of water using **1b** as the catalyst (Tables 2 and 3). The primary products of this reaction were methyl formate and H_2; the latter was identified using gas chromatography (GC) (see Supporting Information Figure

DOI: 10.1021/acscatal.5b00137
ACS Catal. 2015, 5, 2404–2415

Table 2. Solvent Screen for MeOH Dehydrogenation Catalyzed by 1b[a]

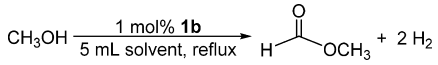

solvent	time[b] (min)	TON[c]	yield (%)
dioxane	20	53	26
propylene carbonate	20	71	35
chlorobenzene	10	80	40
dimethyl sulfoxide	11	96	48
tetrahydrofuran	12	107	53
cyclopentylmethyl ether	10	112	56
toluene	15	116	58
acetonitrile	10	170	85
ethyl acetate	10	176	88

[a]Reaction conditions: MeOH (36 μL, 0.91 mmol), **1b** (9.1 μmol, 1 mol %) 5 mL solvent, reflux. [b]Time at which no further increase in TON was observed. [c]TON was measured using a gas buret. Each equivalent of H_2 generated is counted as a TON. All numbers are the average of two runs.

Table 3. Catalyst Optimization for MeOH Dehydrogenation[a]

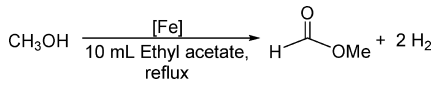

catalyst	mol % [Fe]	time (min)[b]	TON[c]	yield (%)
1a	0.1	50	1460	73
1b	0.1	45	1421	71
C	0.1	40	384	19
2a	0.1	25	255	12
2a + 10 mol % $LiBF_4$	0.1	40	>1999	>99
2b	0.1	30	126	6
2b + 10 mol % $LiBF_4$	0.1	45	1920	96
2a + 10 mol % $LiBF_4$	0.01	265	>19999	>99
2a + 10 mol % $LiBF_4$	0.001	340	12400	6

[a]Reaction conditions: MeOH (36 μL, 0.91 mmol), [Fe] (0.001−0.1 mol %), 10 mL of ethyl acetate, reflux. [b]Time at which no further increase in TON was observed. [c]TON was measured using a gas buret. Each equivalent of H_2 generated is counted as a TON. All numbers are the average of two runs.

S10). High yields of methyl formate were obtained only when the moderately polar solvents ethyl acetate and acetonitrile were utilized (Table 2). In contrast, excellent yields were previously obtained for the dehydrogenation of 1-butanol in nonpolar toluene.[10e] The reasons for the excellent performance in ethyl acetate and acetonitrile, and the relatively low yield for MeOH dehydrogenation in nonpolar solvents such as toluene are unclear. In subsequent optimization reactions, ethyl acetate was used as the solvent because there is a significant decrease in catalytic activity when formic acid dehydrogenation catalyzed by **1** is performed in acetonitrile, which therefore is not a suitable solvent for full aqueous phase MeOH dehydrogenation (see Table S1). The dehydrogenation of MeOH was dependent not only on the identity of solvent but also on the concentration (see Table S2). Dilution studies indicate that the reaction fails at high concentrations. This is consistent with a bimolecular catalyst decomposition pathway, and single crystals of the Fe(0) complex ($^{Cy}PN^HP$)Fe(CO)$_2$, which is proposed to form in a bimolecular fashion, were obtained from a completed catalytic reaction mixture (see Figure S16).

Under the optimized conditions shown in Table 3, **1a** and **1b** show nearly identical activities for MeOH dehydrogenation to methyl formate, giving 73% (1460 turnovers) and 71% yield (1421 turnovers), respectively. To the best of our knowledge these are the highest turnovers reported to date for this reaction.[7,11] Interestingly, the borohydride complex **C** is significantly less active, achieving only 19% yield (384 turnovers). This is consistent with recent observations by Guan and co-workers suggesting that the activation of **C** through loss of BH_3 results in increased catalytic activity for the hydrogenation of esters to alcohols by rapidly generating the active catalyst **1a**.[12] In our current system there is no additive to facilitate the formation of the active species. Presumably, one of the roles of KOH in Beller's aqueous phase dehydrogenation of MeOH using **C**[8c] is to facilitate catalyst activation through the removal of BH_3. The formate complexes **2a** and **2b** are also poor catalysts for MeOH dehydrogenation. This is most likely due to the inability of these species to readily undergo decarboxylation and 1,2-elimination of H_2 to access catalytically active **1a** or **1b**, in the absence of base or LA.[10d]

Recently we demonstrated that LA co-catalysts assist in the dehydrogenation of formic acid using **1a** and **1b**.[10d] The addition of 10 mol % $LiBF_4$ did not influence the yield or kinetic profile for the dehydrogenation of MeOH to methyl formate using **1b** (see Table S3), suggesting that the rate-determining steps in MeOH dehydrogenation and formic acid dehydrogenation are not equivalent. Furthermore, the kinetic isotope effect (KIE) for catalytic MeOH dehydrogenation (determined from rate constants for parallel reactions using MeOH and d_4-MeOH and **1b**, see the Supporting Information) is k_H/k_D = 2.5(2). In contrast, for catalytic formic acid dehydrogenation using **1b** the KIE is k_H/k_D = 4.2(3) (see the Supporting Information). This indicates that the rate-determining steps in the two processes are not an identical elementary reaction, such as H_2 elimination. Although the addition of LA co-catalysts did not enhance catalysis using **1a** and **1b**, a remarkable increase was observed in the cases of **2a** and **2b** (Table 3). In the presence of 10 mol % $LiBF_4$ complete conversion of MeOH to methyl formate was observed using 0.1 mol % **2a** and the catalyst loading could be decreased to 0.01 mol % without any loss in yield.[13] We believe that this dramatic increase occurs because $LiBF_4$ facilitates the decarboxylation of the formate complexes to access the catalytically active species.[10d] The combination of **2** and a LA may provide an alternative strategy for dehydrogenating challenging organic substrates[10e] such as 1-cyclohexylmethanol using low catalyst loading, as it appears to generate a more stable catalytic system than using **1** without any additives.

To further probe the mechanism of MeOH dehydrogenation, stoichiometric reactions were performed (Scheme 3). When 1 equiv of MeOH was added to a d_8-toluene solution of **1b** at low temperature (−80 °C), a new PNP-supported Fe species, **3b**, was observed by ^{1}H and ^{31}P NMR spectroscopy along with **1b** (see Figures S3 and S4). Compound **3b** has a triplet resonance in the ^{1}H NMR spectrum at −23.95 ppm and a singlet resonance in the ^{31}P{^{1}H} NMR spectrum at 84.8 ppm. It is assigned as ($^{Cy}PN^HP$)Fe(CO)(H)(OCH$_3$), which arises from 1,2-addition of MeOH to **1b**. Further evidence for this assignment was obtained through an experiment between CD_3OD and **1b** at −75 °C (see Figure S5). In this reaction two resonances in a 3:1 ratio were observed at 3.57 and 2.04 ppm in the ^{2}H NMR spectrum, along with the previously observed resonance at 84.8 ppm, in the ^{31}P{^{1}H} NMR spectra. The

DOI: 10.1021/acscatal.5b00137
ACS Catal. 2015, 5, 2404−2415

Scheme 3. Stoichiometric Reactions of 1b with MeOH and/or Water

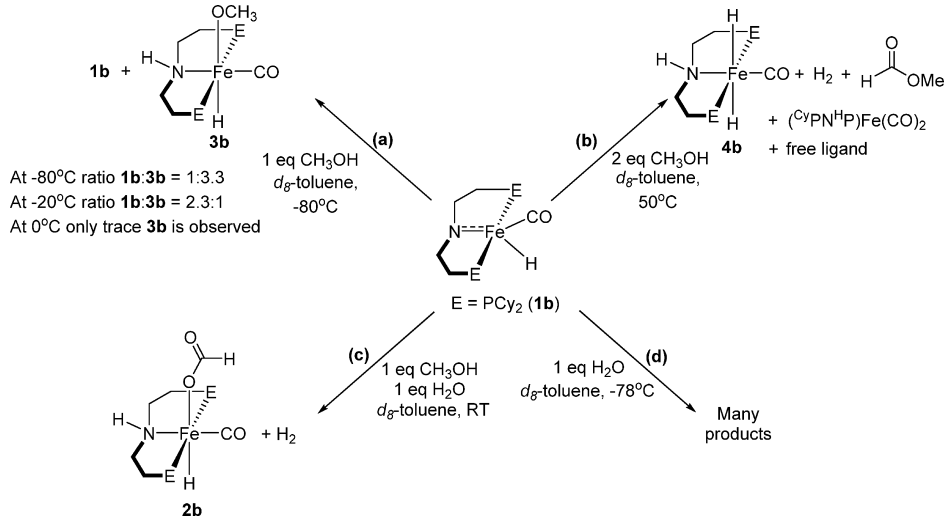

resonances in the ^{2}H NMR spectrum are proposed to correspond to the OCD_3 ligand (3.57 ppm) bound to Fe and the N−D (2.04 ppm) moiety. Free CD_3OD was also observed in the ^{2}H NMR spectrum, which is consistent with the presence of unreacted **1b**. In both experiments using CH_3OH and CD_3OD, the amount of **3b** decreased relative to the amount of **1b** as the temperature was increased. In fact, at 0 °C only trace amounts of **3b** were observed by ^{1}H NMR or ^{2}H NMR spectroscopy and the predominant species is **1b**. Cooling the solutions to −80 °C resulted in the conversion of **1b** and CH_3OH/CD_3OH back to **3b**. These experiments suggest that **1b** and MeOH are in equilibrium with **3b** and that the 1,2-addition of MeOH is temperature dependent. It was not possible to isolate **3b**, as the removal of solvent resulted in the regeneration of **1b**, along with substantial amounts of free ligand and unidentified solid precipitate.

When the reaction between 1 equiv of MeOH and **1b** in d_8-toluene was performed at 50 °C, there was no evidence for the formation of **3b**. Instead, the major Fe-containing products were the dihydride $(^{Cy}PN^HP)Fe(CO)(H)_2$ (**4b**), which we previously characterized,[10d] and $(^{Cy}PN^HP)Fe(CO)_2$. Also present were a significant amount of free ligand, H_2, methyl formate, and MeOH (see Figures S6 and S7). The analogous reaction between **1b** and 2 equiv of MeOH (Scheme 3b) resulted in the formation of the same products, but no MeOH was observed. We believe that the pathway for this reaction involves initial dehydrogenation of MeOH to produce formaldehyde and H_2 followed by esterification of formaldehyde with MeOH to form methoxymethanol, which is subsequently dehydrogenated to generate methyl formate and the second equivalent of H_2 (Scheme 4). This is the same sequence of reactions previously proposed for butanol dehydrogenation[10e] and is consistent with our catalytic results. The observation of the dihydride complex **4b** suggests that release of H_2 to regenerate **1b** is slow and is in agreement with the observation that **4b** is the resting state during catalysis as determined using ^{31}P NMR spectroscopy.

Scheme 4. Proposed Stepwise Pathway for MeOH Dehydrogenation in the Absence of Water

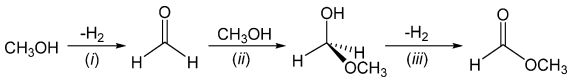

In the reaction pathway shown in Scheme 2, water is necessary to fully dehydrogenate MeOH and generate 3 equiv of H_2. The stoichiometric reaction of **1b** with 1 equiv of both MeOH and water led to the formation of the previously characterized formate complex **2b** along with H_2.[10d] A proposed pathway for this reaction is summarized in Scheme 5. Initially, MeOH is dehydrogenated by **1b** to generate formaldehyde and H_2, with the latter presumably formed via the dihydride intermediate **4b**. Subsequently, formaldehyde is trapped by water to form methanediol, which is dehydrogenated to form formic acid and **4b**. Formic acid then protonates **4b** to form H_2 and the formate product **2b**. There is precedent for all of the steps in this reaction sequence.[10d,e] In a control experiment, **1b** was treated with 1 equiv of water (Scheme 3d). Even at low temperature a large number of different products were observed by ^{31}P NMR spectroscopy, none of which were identifiable. Furthermore, removal of the solvent led to almost complete decomposition of the complexes, with only a small amount of **1b** recovered, indicating that the addition of water is largely irreversible. This strongly suggests that when both water and MeOH are present, **1b** initially reacts with MeOH.

Scheme 5. Proposed Pathway for Stoichiometric Reaction of 1 equiv of MeOH and Water with 1b

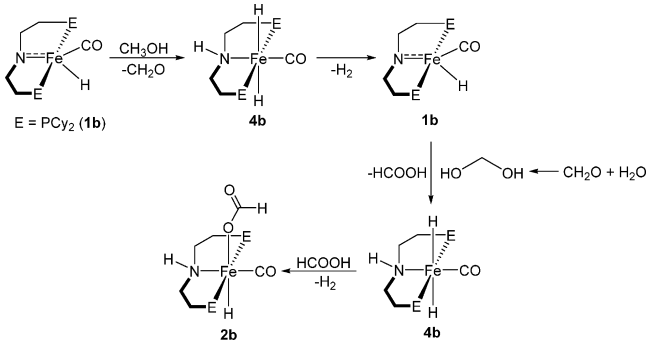

Aqueous Phase MeOH Dehydrogenation. Given the similarity of **1** to Beller's catalyst, **C**, we began our investigation

DOI: 10.1021/acscatal.5b00137
ACS Catal. 2015, 5, 2404−2415

of aqueous phase MeOH dehydrogenation using Beller's optimized conditions of 4:1 (molar ratio) MeOH/H_2O.[8c] In the absence of a base or other additive, **1b** catalyzes the generation of H_2 from an aqueous solution of MeOH in 58% yield, based on water as the limiting reagent (Table 4). However, methyl formate is also generated as a significant product, suggesting that complete MeOH dehydrogenation to H_2 and CO_2 is not occurring. When this reaction was monitored using ^{31}P NMR spectroscopy, the major Fe-containing species at the end of the reaction was the formate complex **2b**. Presumably, if **2b**, which we believe is formed through 1,2 addition of formic acid to **1b** (vide supra), cannot undergo facile decarboxylation, it represents a highly stable intermediate in catalysis. To prevent the accumulation of **2b**, the catalytic reaction was performed in the presence of a variety of different LAs (Table 4). Several different LAs facilitate the complete aqueous phase dehydrogenation of MeOH, without formation of methyl formate. In general, the smaller, more oxophilic cations such as Li^+ and Na^+ are the most active. Additionally, non-coordinating or weakly coordinating anions are necessary, with PF_6^-, BF_4^-, and OTf^- giving the best results. It is possible to use LAs as simple as NaCl, but the poisoning effect of the chloride anion appears to be similar regardless of the cation, as there is little difference in activity between LiCl, NaCl, and CsCl. Even in the presence of LAs, ^{31}P NMR spectroscopy indicates that the formate complex **2b** is the resting state during catalysis.

The six LAs that gave quantitative conversion of MeOH and water to H_2 and CO_2 at 0.5 mol % loading of **1b** were tested at lower catalyst loading to further explore the differences in their activities (see Table S4). Despite their impressive performances at high catalyst loading, both LiOTf and NaOTf performed poorly under these conditions, whereas $LiBF_4$ was the most active, giving >99% yield in 12.5 h. The gas produced from the reaction using $LiBF_4$ was analyzed by GC and found to contain a 3:1 ratio of H_2/CO_2 and <0.1% CO (see Figures S12−S15). This percentage of CO is significantly lower than that observed with the best current heterogeneous catalysts[3a,6a] and comparable with state-of-the art precious metal homogeneous systems.[8a,b] Using $LiBF_4$ as the LA, we explored the effect of changing the quantity of LA on TON (Table 5). When the catalyst loading of **1b** is 0.5 mol %, the optimal LA loading is between 5 and 10 mol %; however, at a lower loading of **1b** (0.1 mol %), a 10 mol % LA loading gives more efficient catalytic activity. The decrease in performance at both higher and lower LA loading is comparable to the LA effect that was observed in formic acid dehydrogenation using **1** and **2**.[10d]

The effect of changing the ratio of MeOH/H_2O was explored using a catalyst system including **1b** and $LiBF_4$ (Table 6). A large excess of either MeOH or water afforded poor yields. More moderate ratios of 2:1 or 4:1 MeOH/H_2O gave significantly higher TON and yields, with a ratio of 4:1 giving a TON of 9500 (95% yield) in 41 h. The significant decrease in catalytic activity at high water and/or MeOH concentrations may be related to the instability of **1b** in either neat MeOH or water. This is in contrast to the reaction of **1b** with 1 equiv of a mixture of MeOH and water, which gave near quantitative conversion to **2b**, with very little evidence of decomposition. Our optimal conditions are similar to those employed by Beller and co-workers to achieve a TON of approximately 10 000 in 43 h using **C** and 8 M KOH.[8c]

Using our optimized conditions we tested the catalytic activity of **1a**, **1b**, **2a**, **2b**, and **C** (Table 7). In combination with $LiBF_4$, both the amido complexes **1a** and **1b** and the formate complexes **2a** and **2b** give yields >80% (8000 turnovers) at 0.03 mol % catalyst loading. In an analogous fashion to the dehydrogenation of MeOH to methyl formate, **C** is not highly active under these base-free conditions, giving only 25% yield. This is presumably because it is not efficiently activated. Further optimization using **2a** at 0.01 mol % loading gave a TON of 30 000 and yield of >99%. Lowering the catalyst loading to 0.006 mol % gave a TON of 51 000, but the yield was reduced to 50%. Overall, **2b** in combination with 10 mol % $LiBF_4$ represents the first example of base-free MeOH

Table 4. LA Screening for Aqueous Phase MeOH Dehydrogenation Using 1b[a]

$CH_3OH + H_2O$ (4:1) —[0.5 mol% **1b**, 10 mol% LA, 10 mL Ethyl acetate, reflux]→ $3\,H_2 + CO_2$

LA	TON[b] (time, min)[c]	yield[d] (%)	LA	TON[b] (time, min)[c]	yield[d] (%)
no additive	350 (20)	58[e]	NaCl	497 (15)	82
			LiCl	499 (15)	83
$LiPF_6$	>599 (30)	>99	KCl	496 (25)	82
$NaPF_6$	425 (20)	70	CsCl	427 (15)	71
KPF_6	>599 (35)	>99	$CaCl_2$	297 (10)	49
$LiBF_4$	>599 (25)	>99	$NaBAr^F{}_4$[f]	>599 (20)	>99
$NaBF_4$	542 (20)	90	$NaBPh_4$	410 (15)	68
KBF_4	530 (30)	88	$NaBF_4$	542 (20)	90
LiOTf	>599 (15)	>99			
NaOTf	>599 (35)	>99			
KOTf	393 (20)	65			

[a]Reaction conditions: water (18 μL, 1.0 mmol), MeOH (161 μL, 4.0 mmol), **1b** (0.5 mol % with respect to water), LA (0.1 mmol, 10 mol % with respect to water), 10 mL of ethyl acetate, reflux. [b]TON measured using a gas buret. Each equivalent of H_2 generated is counted as a TON. All numbers are the average of two runs. [c]Time at which no further increase in TON was observed. [d]Based on water as the limiting reagent. [e]Methyl formate was observed as a major product. [f]$BAr^F{}_4$ = $B\{3,5\text{-}(CF_3)_2C_6H_3\}_4^-$.

Table 5. Effect of Amount of $LiBF_4$ on MeOH Dehydrogenation in the Presence of Water[a]

$CH_3OH + H_2O$ (4:1) —[**1b**, $LiBF_4$, 10 mL Ethyl acetate, reflux]→ $3\,H_2 + CO_2$

mol % LA	mol % **1b**	time (min)[b]	TON[c]	yield (%)
1	0.5	25	350	58
2		25	375	62
5		20	>599	>99
10		25	>599	>99
20		60	>599	>99
5	0.1	320	975	32
10		600	>2999	>99
20		750	>2999	>99

[a]Reaction conditions: water (18 μL, 1.0 mmol), MeOH (161 μL, 4.0 mmol), **1b** (*x* mol % with respect to water), LA (mol % with respect to water),10 mL of ethyl acetate, reflux. [b]Time at which no further increase in TON was observed. [c]TON measured using a gas buret. Each equivalent of H_2 generated is counted as a TON. All numbers are the average of two runs.

DOI: 10.1021/acscatal.5b00137
ACS Catal. 2015, 5, 2404−2415

Table 6. Effect of MeOH/H_2O Ratio on MeOH Dehydrogenation in the Presence of Water Using 1b[a]

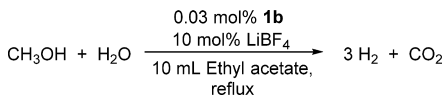

MeOH/H_2O (M)	time[b] (h)	TON[c]	yield (%)
8:1	4	500	5
6:1	30	2780	28
4:1	41	9500	95
2:1	38	6000	60
1:1	5.5	5000	50
1:2	2.5	604	6

[a]Reaction conditions: water (18 μL, 1.0 mmol), appropriate molar quantity MeOH, **1b** (0.03 mol % with respect to water), $LiBF_4$ (0.10 mmol, 10 mol %), 10 mL of ethyl acetate, reflux. [b]Time at which no further increase in TON was observed. [c]TON was measured using a gas buret. Each equivalent of H_2 generated is counted as a TON. All numbers are the average of two runs.

Table 7. Screening of Catalysts for MeOH Dehydrogenation in the Presence of Water[a]

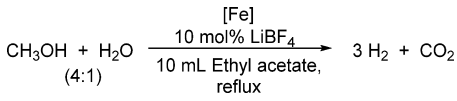

catalyst	mol % [Fe]	time[b] (h)	TON[c]	yield (%)
1a	0.03	42	8200	82
1b	0.03	41	9500	95
C	0.03	21	2500	25
2a	0.03	39	>9999	>99
2b	0.03	41	>9999	>99
2a	0.01	52	30,000	>99
2a	0.006	94	51,000	50

[a]Reaction conditions: water (18 μL, 1.0 mmol), MeOH (160 μL, 4.0 mmol), [Fe], $LiBF_4$ (0.10 mmol, 10 mol %),10 mL of ethyl acetate, reflux. [b]Time at which no further increase in TON was observed. [c]TON measured using a gas buret. Each equivalent of H_2 generated is counted as a TON. All numbers are the average of two runs.

dehydrogenation by a first-row metal, giving 5 times greater turnover than previous Fe catalysts and 12 times better turnover than other base-free systems.

It is surprising that the formate complexes **2a** and **2b** give slightly superior yields and reach completion more rapidly for both MeOH dehydrogenation in the absence of water and aqueous phase MeOH dehydrogenation, even though it is proposed that they need to access **1a** or **1b**, respectively, for productive catalysis to occur. Our explanation for this strange observation is that the five coordinate species **1** undergo nonproductive side reactions with MeOH and water at room temperature. For example, we have already demonstrated the facile 1,2-addition of MeOH to **1b** at low temperature, which we do not believe leads to dehydrogenation (vide infra) and results in some decomposition. Thus, in catalysis using the five coordinate species, these unproductive side reactions deactivate some of the catalyst before MeOH dehydrogenation can initiate. In contrast, the formate complexes **2** are less prone to these side reactions because the Fe center must first undergo decarboxylation, which typically only occurs at temperatures at which MeOH dehydrogenation is also operative.[10d] Furthermore, at the elevated temperatures at which decarboxylation occurs, 1,2-addition of MeOH is no longer preferred, so once **1** is formed, it does not decompose so rapidly. Support for this hypothesis was obtained from the following experiment: the addition of an excess of a 4:1 molar mixture of MeOH/H_2O to an ethyl acetate solution containing **1b** and $LiBF_4$ at room temperature led to the formation of some free ligand, indicative of catalyst decomposition (see the Supporting Information). In contrast, no reaction occurred using **2b** under the same conditions.

Mechanistic Studies. DFT calculations were performed to provide further insight into the mechanism of aqueous phase MeOH dehydrogenation using **1**. We employed smaller model Fe complexes in the calculations by replacing the isopropyl or cyclohexyl groups of the phosphine ligands with methyl substituents. It has previously been demonstrated that this change has only a minor effect on the energetics of PNP supported Fe complexes.[10e] The relative free energies reported below were obtained at the B3LYP/def2-SVP level of DFT and relate to standard conditions (gaseous species at 298 K and 1 bar). Our chosen level of DFT was validated by comparison to coupled-cluster single-point results obtained at the extrapolated basis-set limit, CCSD(T)/CBS(T,Q), for a set of minima and transition structures representative of the system under study (see Figure S17). The benchmarking study indicates sufficient agreement for a qualitative assessment of reaction pathways, which is our aim here, but with a maximum deviation of about 6 kcal mol^{-1} for relative electronic energies, our expectations as to a quantitative description are limited. In our computational study we explore pathways for full aqueous phase dehydrogenation of MeOH along the four-step reaction sequence depicted in Scheme 2. Accordingly, we discriminate between four individual reaction sequences in the following discussion of the computational results: (A) MeOH dehydrogenation, (B) hemiacetal formation, (C) methanediol dehydrogenation, and (D) formate dehydrogenation. Stationary points identified along the individual routes are denoted correspondingly by preceding capital letters; please note that the numbering scheme deviates from that used in the Experimental Section.

The first step in the dehydrogenation of MeOH is the formation of formaldehyde and 1 equiv of H_2. The lowest energy pathway for this process is shown in Scheme 6. Initially, an encounter complex **A2** is formed via an N···H···O hydrogen bond between MeOH and the five-coordinate amido species **A1**. Subsequently, concerted transfer of the hydrogen atoms associated with both the C−H and O−H bonds occurs to generate **A4** (corresponding to **4a** or **4b** discussed above) and formaldehyde, via an intermediate encounter complex **A3**. The barrier for this process via **TS-A2** is relatively low (15 kcal mol^{-1} relative to MeOH and **A1**), and this reaction sequence is analogous to the calculated first step in the conversion of alcohols to esters and 2 equiv of H_2, which was previously reported by our group using **1a**.[10e] This pathway is also closely related to that proposed by Grützmacher and co-workers for the dehydrogenation of ethanol to acetaldehyde using a Rh system, although in this case it is proposed that the O−H bond is cleaved before the C−H bond.[14] Yang[15] in turn, calculated a stepwise ionic pathway for the dehydrogenation of ethanol to acetaldehyde using **1a**.[16] An alternative pathway for the reaction of MeOH and **A1** to generate formaldehyde and **A4**, involving 1,2-addition of MeOH across the Fe−N bond to generate an alkoxide followed by β-hydride elimination, was calculated to be significantly higher in energy (see Figure S20). However, initial 1,2-addition of MeOH was slightly energetically favored, consistent with our experimental observation of the alkoxide

DOI: 10.1021/acscatal.5b00137
ACS Catal. 2015, 5, 2404−2415

Scheme 6. Calculated Lowest Free Energy Pathway for MeOH Dehydrogenation (A)

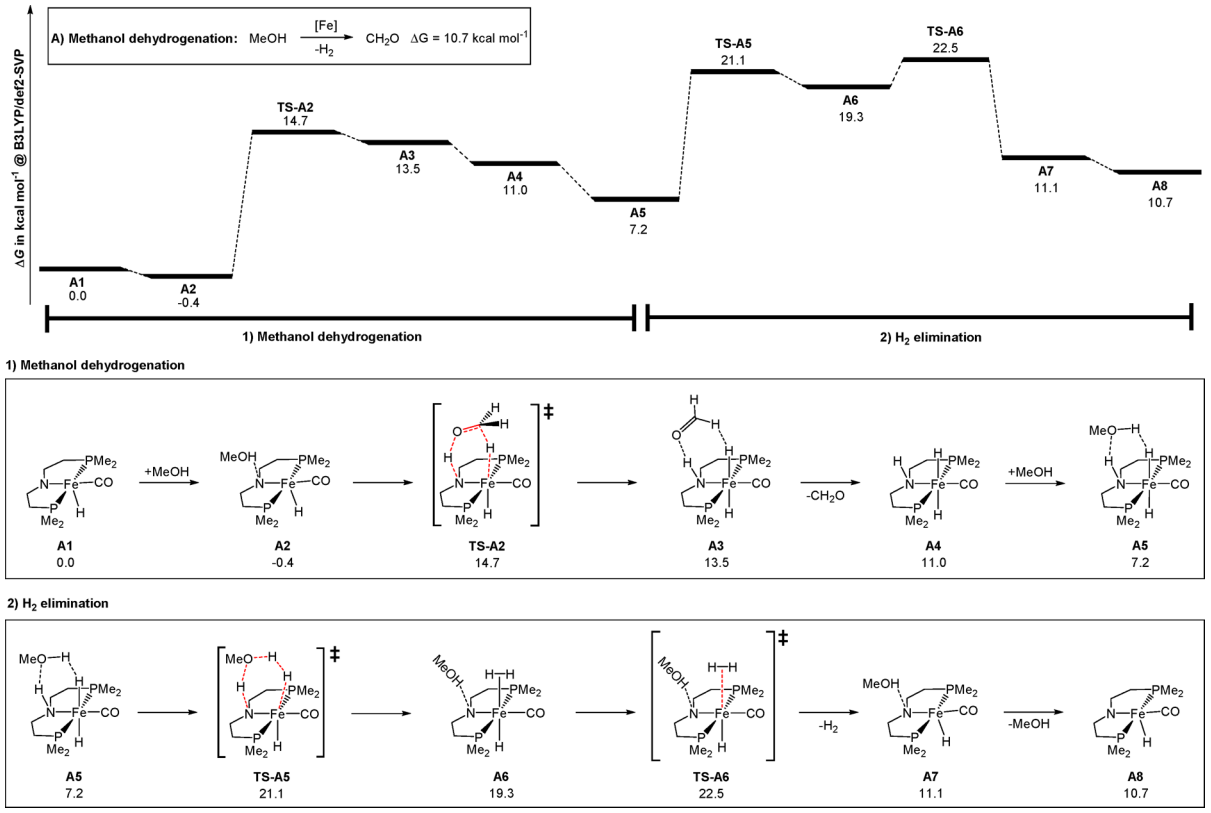

Scheme 7. Calculated Pathways for Conversion of Formaldehyde and Water into Methanediol (B)

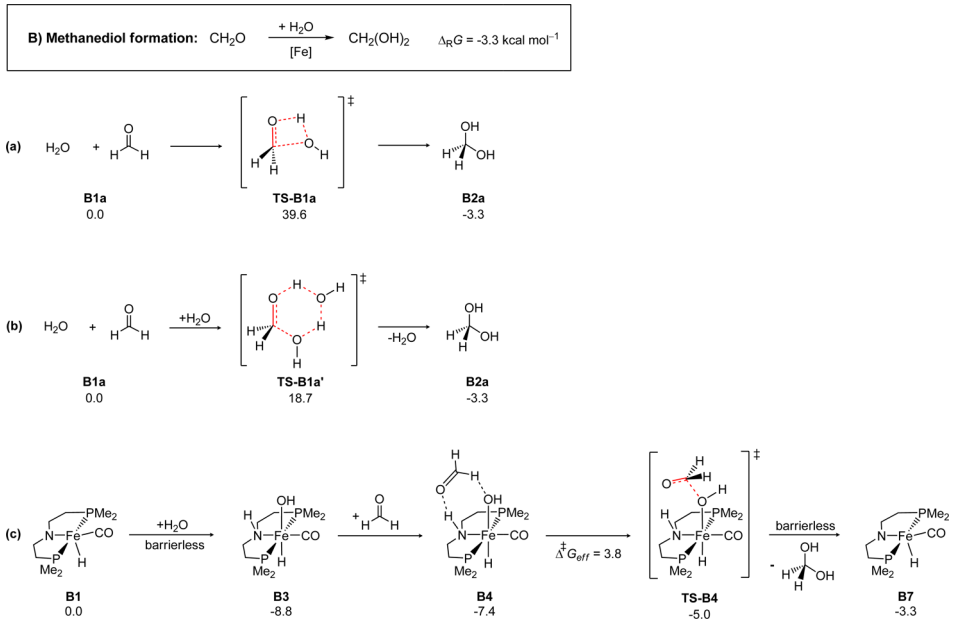

complex **3b** at low temperature (vide supra). The loss of dihydrogen from **A4** to regenerate **A1** is mediated by MeOH and, with a barrier of 23 kcal mol^{-1}, represents the rate-determining step in the conversion of MeOH to formaldehyde and H_2. We have previously described this process for H_2 elimination in detail.[10e] The barrier for H_2 elimination is higher when mediated by water compared to MeOH (see Figure S21). In line with expectation, we find that the thermodynamic favorability of H_2 loss from **A4** to form **A1** varies as a function of the H_2 pressure (see Figure S18), consistent with experimental results on the stability of **4a**/**4b**.[10d]

Recently, both our group[10e] and Azofra et al.[17] reported that there was a large barrier to uncatalyzed hemiacetal formation from MeOH and formaldehyde. Similarly, the barrier to uncatalyzed methanediol formation from MeOH and water is also high (40 kcal mol^{-1}, Scheme 7a). A pathway in which a second molecule of water acts as a shuttle is significantly lower in energy, with a barrier of 19 kcal mol^{-1} for the six-membered

DOI: 10.1021/acscatal.5b00137
ACS Catal. 2015, 5, 2404−2415

Scheme 8. Calculated Lowest Free Energy Pathway for Methanediol Dehydrogenation (C)

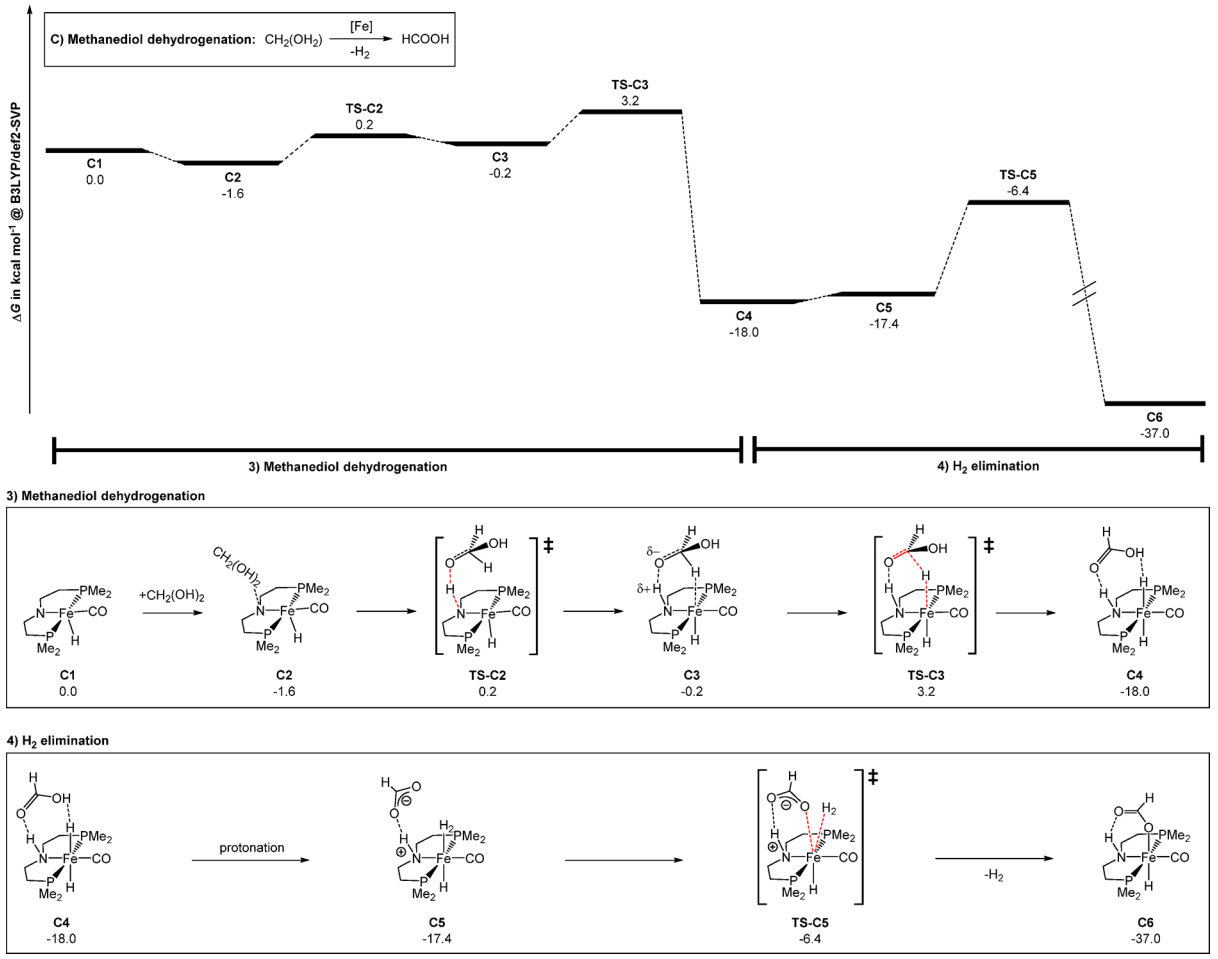

transition state (Scheme 7b). However, the lowest energy pathway for methanediol formation is mediated by **B1** (Scheme 7c). It involves initial 1,2-addition of water across the Fe−N bond to generate the hydroxide complex (**B3**, similar to **3b** discussed under Experimental Section). This species forms an encounter complex with formaldehyde (**B4**), which facilitates the formation of the new C−O and O−H bonds, via a low-energy transition state (**TS-B4**, 4 kcal mol^{-1}). The facile calculated pathway for 1,2-addition of water to **B1** is consistent with our experimental observation that **1** reacts rapidly with water (Scheme 3), although we were unable to identify any well-defined products in the experiments. In analogy to our results, Grützmacher and co-workers reported a closely related, low-barrier pathway for the corresponding reaction mediated by a Rh system.[14]

The third step in the overall process is the dehydrogenation of methanediol (Scheme 8). The initial approach of methanediol to **C1** is similar to that described for MeOH, with an encounter complex **C2**, formed via an N···H···O hydrogen bond. However, the subsequent dehydrogenation occurs through a stepwise rather than a concerted pathway. Initially, the amido ligand is protonated by methanediol to form intermediate **C3**. Subsequent transfer of the hydrogen atom associated with one of the C−H bonds of methanediol generates **C4**, an encounter complex between formic acid and the dihydride complex. Formic acid, which is the strongest acid generated in the reaction cascade, then protonates an Fe−H bond in **C4** to form **C5**, a cationic molecular H_2 complex stabilized by a formate ion. The whole reaction cascade **C1** → **C5** occurs without significant activation barriers, and also the subsequent displacement of the coordinated H_2 ligand by formate to form **C6** has a small barrier only (12 kcal mol^{-1} via **TS-C5**). Overall, methanediol dehydrogenation represents a highly exergonic process (−37 kcal mol^{-1} relative to **C1** or −26 kcal mol^{-1} relative to **A1**).

The final step in aqueous phase MeOH dehydrogenation is the decarboxylation of the formate complex **D1**, followed by release of H_2 to regenerate **D7** (Scheme 9). We have previously demonstrated that in the absence of LA the barrier for the decarboxylation of **D1** is high,[10d] consistent with the experimental observation that a LA is required for this process. We decided to model the effect of the LA on decarboxylation using Na^+.[18] As we have no relevant information on the nature of the Na^+ coordination environment in the rather complex reaction mixture, we chose $Na(H_2O)_6^+$ as a model LA to study its influence on the formate decarboxylation at least in a qualitative fashion. Our calculations predict that expulsion of one water ligand from the coordination sphere of Na^+ and binding of $Na(H_2O)_5^+$ to the formate ligand in **D1** is thermodynamically favorable by −12 kcal mol^{-1} (see Figure S19). This value is almost certainly an overestimation, as experimentally we do not observe significant changes in the NMR properties of the formate complexes when LAs are added and have never isolated a species with a LA coordinated. We hence assume that in reality, a LA adduct of the formate complex is rather approximately isoenergetic with the separated

DOI: 10.1021/acscatal.5b00137
ACS Catal. 2015, 5, 2404−2415

Scheme 9. Lowest Free Energy Pathways in the Absence (Black) and the Presence of LA (Red) for Formic Acid Dehydrogenation (D)

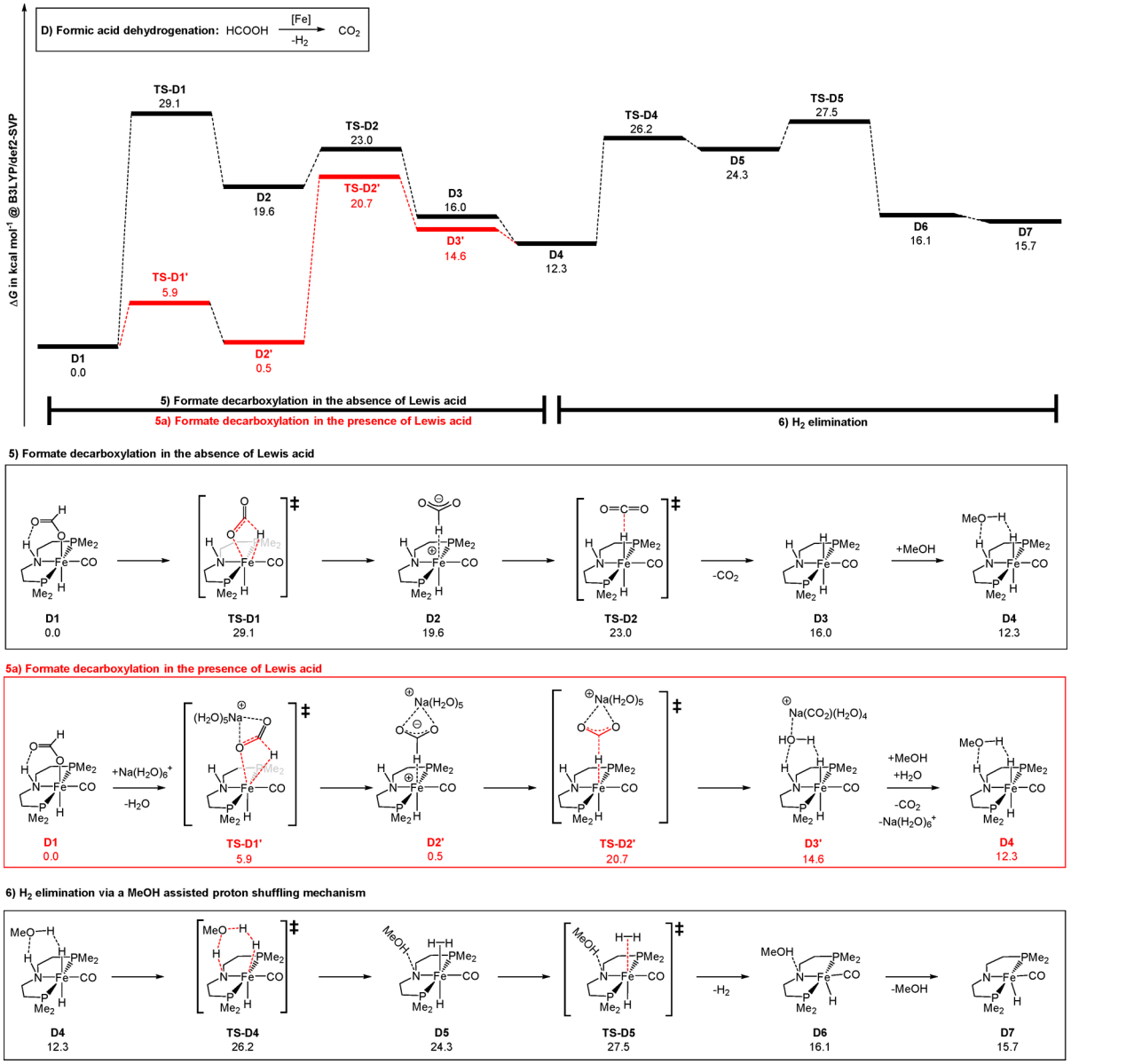

LA and the formate in solution. Nevertheless, as we previously hypothesized,[10d] Na^+ coordination to the formate ligand stabilizes the negative charge that develops in the decarboxylation step, thereby significantly lowering its activation barrier. Correspondingly, we find that both transition states, **TS-D1** and **TS-D2**, and the H-bound formate intermediate **D2** are substantially lowered by LA coordination (Scheme 9).[19] Subsequent release of H_2 from **D3** to regenerate **D7** is then again facilitated by MeOH as described before. In the presence of the LA, the latter step is overall rate limiting for the sequence **D1** → **D7**. In this scenario, there is a pre-equilibrium involving reversible CO_2 insertion/decarboxylation and the formate complex **D1** represents the resting state during catalysis, which is consistent with our experimental observations.

In summary, notwithstanding a number of assumptions made in our theoretical assessment, which certainly limit the expectable accuracy in the description of the realistic process, our calculations provide a qualitative picture of the elementary steps involved in aqueous phase MeOH dehydrogenation (Scheme 10 shows the overall catalytic cycle resulting from our computational study). We have identified the role of the LA in facilitating decarboxylation, and in principle this effect could be transferable to other systems that are proposed to decarboxylate via an outer sphere mechanism. Additionally, LAs may also assist in CO_2 insertion reactions into metal hydrides, which are the microscopic reverse of this outer sphere decarboxylation; however at this stage there are no direct data to support this proposal. Our calculations demonstrate the difficulty associated in 1,2-elimination of H_2 from **4a**/**4b**, and to design improved catalysts based on our Fe systems, it is crucial to reduce the barrier for H_2 elimination. This may result in systems that operate at lower temperature and are more stable, which is necessary to achieve TONs that are comparable to the best precious metal systems.

DOI: 10.1021/acscatal.5b00137
ACS Catal. 2015, 5, 2404−2415

Scheme 10. Overall Catalytic Cycle Computed for Lewis Acid Assisted Methanol Dehydrogenation (Effective Activation Barriers for Key Elementary Steps in kcal mol^{-1}; B3LYP/def2-SVP)

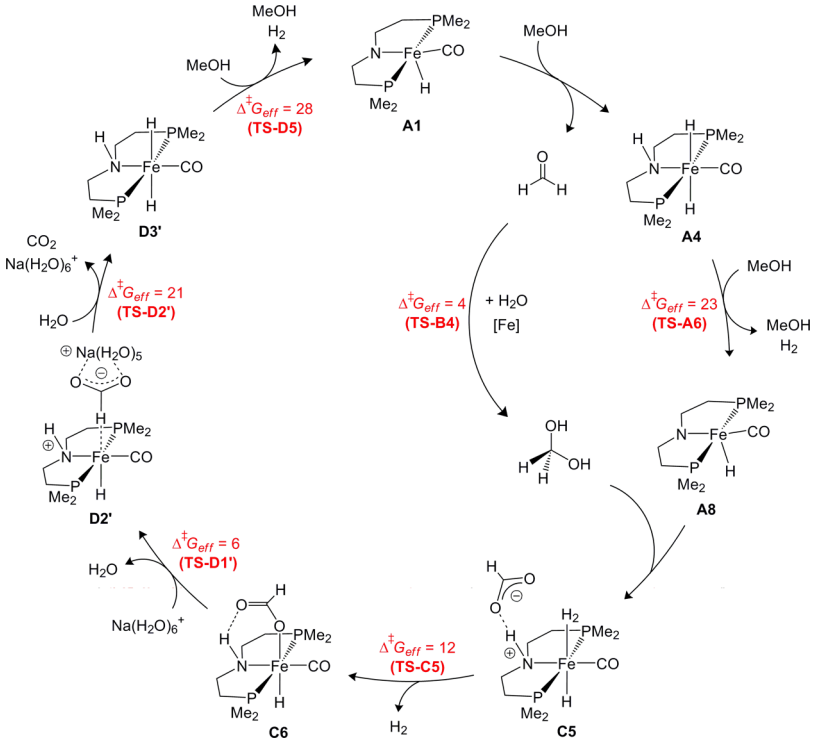

CONCLUSIONS

We have demonstrated that a family of PNP-supported Fe complexes generates highly active catalysts for the dehydrogenation of MeOH. In the absence of water, these catalysts rapidly convert MeOH to methyl formate and H_2. Although a LA is not required for this reaction, the catalytic system that gives the highest TON (approximately 20 000) requires a LA for activation. In the presence of water, our Fe complexes fully dehydrogenate MeOH to H_2 and CO_2, provided a LA co-catalyst is present. For this reaction our best Fe/$LiBF_4$ system gives a TON of approximately 51 000, which is the highest reported to date for a homogeneous first-row transition metal catalyst or a system that does not require a Brønsted base. There are two major advantages to using a LA instead of a Brønsted base: (i) the reaction conditions are milder, which could both extend catalyst lifetime and increase the potential range of improved catalysts that could be developed in the future; and (ii) the loading of LA required is significantly lower than the loading of base typically used. The mechanism of MeOH dehydrogenation is proposed to involve four steps: (i) initial dehydrogenation of MeOH to formaldehyde; (ii) reaction of water with formaldehyde to form methanediol; (iii) dehydrogenation of methanediol to form an Fe formate species and H_2; and (iv) decarboxylation of the Fe formate species to release CO_2 and the final equivalent of H_2. The LA is required to facilitate the decarboxylation of the Fe formate species, whereas the ability of the PNP ligand to undergo bifunctional reactivity is crucial to many of the elementary steps in the reaction pathway. In future work, we will continue to explore the potential of Fe complexes supported by PNP ligands to release H_2 from small molecules with the potential to be used for chemical hydrogen storage.

EXPERIMENTAL SECTION

General Methods. Experiments were performed under a dinitrogen or argon atmosphere in an inert atmosphere glovebox or using standard Schlenk techniques, unless otherwise noted. Under standard inert atmosphere glovebox conditions, purging was not performed between uses of pentane, diethyl ether, benzene, toluene, and THF; thus, when any of these solvents were used, traces of all these solvents were in the atmosphere and could be found intermixed in the solvent bottles. Moisture- and air-sensitive liquids were transferred by stainless steel cannula on a Schlenk line or in an inert atmosphere glovebox. Solvents were dried by passage through a column of activated alumina followed by storage under dinitrogen or argon. Ethyl acetate, propylene carbonate, and dioxane were dried over CaH_2 and distilled before use. All commercial chemicals were used as received, except where noted. Lithium hexafluorophosphate, sodium hexafluorophosphate, potassium hexafluorophosphate, lithium triflate, sodium triflate, potassium triflate, and sodium tetraphenylborate were purchased from Fisher Scientific Co. Sodium chloride, lithium chloride, potassium chloride, cesium chloride, calcium chloride, lithium tetraphenylborate, sodium tetraphenylborate, and potassium tetraphenylborate were purchased from Acros. Deuterated solvents were obtained from Cambridge Isotope Laboratories. d_8-Toluene was dried over sodium metal and vacuum-transferred prior to use. Literature procedures were used to prepare sodium tetrakis[(3,5-trifluoromethyl)phenyl]borate ($NaBAr^F_4$),[20] **1a**,[10d] **1b**,[10d] **2a**,[10d] **2b**,[10d] and **C**.[9] NMR spectra were recorded on Bruker AMX-400, AMX-500, and AMX-600 spectrometers at ambient probe temperatures, unless otherwise noted.

Computational Details. DFT calculations were performed using the Gaussian 09 program package.[21] The B3LYP hybrid functional,[22] as implemented in Gaussian 09, was used in combination with the def2-SVP basis set.[23] Unscaled zero-point vibrational energies as well as thermal and entropic corrections were obtained from computed Hessians using the standard procedures implemented in Gaussian 09 and were used to obtain Gibbs free energies at 298.15 (1 bar atmospheric pressure).

DOI: 10.1021/acscatal.5b00137
ACS Catal. 2015, 5, 2404−2415

Gas Chromatography. Gas chromatography experiments were performed on a Buck Scientific 910 gas chromatograph with FID/TCD and methanizer. The system uses N_2 as a carrier gas and allows for the determination of the following gases and detection limits: $H_2 \geq 100$ ppm, CO ≥ 1 ppm, and $CO_2 \geq 1$ ppm.

Representative Procedure for Catalytic MeOH Dehydrogenation in the Presence and Absence of Water. In an inert atmosphere glovebox, a 50 mL Schlenk flask was loaded with the appropriate catalyst, MeOH, additive (LA), water (for aqueous phase reactions), and the desired solvent. The Schlenk flask was sealed with a glass stopper and removed from the inert atmosphere glovebox and attached to a gas buret setup and reflux condenser (see Figure S1). The gas buret and tubing was subjected to three vacuum/N_2 purge cycles and allowed to equilibrate. For aqueous phase reactions the U-tube trap was cooled with liquid nitrogen. The solution flask was then lowered into an oil bath preheated to the desired temperature upon which gas evolution began immediately. The change in water level in the gas buret (V_{obs}) was used to determine turnover using previously reported methods (see Figure S1).[8c,10d] Each equivalent of H_2 produced was taken to be one turnover. For aqueous phase reactions, upon completion of the reaction, the U-tube was removed from the liquid nitrogen bath and the CO_2 gas evolved was measured by the buret to be a third of total turnover. In all cases, a blank reaction was run in which no catalyst was added to the solution. The volume of gas obtained from this reaction (trace solvent and MeOH) was recorded as V_{blank}.

■ ASSOCIATED CONTENT

Supporting Information

The following files are available free of charge on the ACS Publications website at DOI: 10.1021/acscatal.5b00137.

Further experimental details, X-ray information for ($^{Cy}PN^{H}P$)Fe(CO)$_2$, and details of DFT calculations (PDF)

CIF format data (CIF)

■ AUTHOR INFORMATION

Corresponding Authors

*(W.H.B.) E-mail: wesley_bernskoetter@brown.edu.

*(N.H.) E-mail: nilay.hazari@yale.edu.

*(M.C.H.) E-mail: max.holthausen@chemie.uni-frankfurt.de.

Notes

The authors declare no competing financial interest.

■ ACKNOWLEDGMENTS

W.H.B. and N.H. thank the National Science Foundation for support through Grant CHE-1240020, a Center for Chemical Innovation. M.C.H. acknowledges support through the COST Action 1205 (CARISMA). Calculations were performed at the Center for Scientific Computing (CSC) Frankfurt on the FUCHS and LOEWE-CSC high-performance compute clusters. N.H. and W.H.B. are fellows of the Alfred P. Sloan Foundation, and N.H. is a Camille and Henry Dreyfus Foundation Teacher Scholar. We are grateful to Professor Sven Schneider for valuable discussions, Steven Ahn for help with GC, and Dr. Brandon Mercado for assistance with crystallography.

■ REFERENCES

(1) (a) Dincer, I. *Energy Policy* **1999**, *27*, 845−854. (b) Lewis, N. S.; Nocera, D. G. *Proc. Natl. Acad. Sci. U.S.A.* **2006**, *103*, 15729−15735.

(2) (a) Bockris, J. O. M. *Science* **1972**, *176*, 1323. (b) Bockris, J. O. M. *Int. J. Hydrogen Energy* **2002**, *27*, 731−740. (c) Midilli, A.; Ay, M.; Dincer, I.; Rosen, M. A. *Renewable Sust. Energy Rev.* **2005**, *9*, 255−271.

(3) (a) Navarro, R. M.; Pena, M. A.; Fierro, J. L. *Chem. Rev.* **2007**, *107*, 3952−3991. (b) Boddien, A.; Loges, B.; Junge, H.; Beller, M. *ChemSusChem* **2008**, *1*, 751−758. (c) Eberle, U.; Felderhoff, M.; Schuth, F. *Angew. Chem., Int. Ed.* **2009**, *48*, 6608−6630. (d) Staubitz, A.; Robertson, A. P.; Manners, I. *Chem. Rev.* **2010**, *110*, 4079−4124. (e) Grasemann, M.; Laurenczy, G. *Energy Environ. Sci.* **2012**, *5*, 8171−8181. (f) Dalebrook, A. F.; Gan, W.; Grasemann, M.; Moret, S.; Laurenczy, G. *Chem. Commun.* **2013**, *49*, 8735−8751.

(4) Carmo, M.; Fritz, D. L.; Mergel, J.; Stolten, D. *Int. J. Hydrogen Energy* **2013**, *38*, 4901−4934.

(5) (a) Olah, G. A. *Angew. Chem., Int. Ed.* **2005**, *44*, 2636−2639. (b) Olah, G. A. *Angew. Chem., Int. Ed.* **2013**, *52*, 104−107.

(6) (a) Palo, D. R.; Dagle, R. A.; Holladay, J. D. *Chem. Rev.* **2007**, *107*, 3992−4021. (b) Gärtner, F.; Losse, S.; Boddien, A.; Pohl, M.-M.; Denurra, S.; Junge, H.; Beller, M. *ChemSusChem* **2012**, *5*, 530−533. (c) Okamoto, Y.; Ida, S.; Hyodo, J.; Hagiwara, H.; Ishihara, T. *J. Am. Chem. Soc.* **2011**, *133*, 18034−18037.

(7) (a) Itagaki, H.; Saito, Y.; Shinoda, S. *J. Mol. Catal.* **1987**, *41*, 209−220. (b) Morton, D.; Cole-Hamilton, D. J. *J. Chem. Soc., Chem. Commun.* **1987**, 248−249.

(8) (a) Rodríguez-Lugo, R. E.; Trincado, M.; Vogt, M.; Tewes, F.; Santiso-Quinones, G.; Grützmacher, H. *Nat. Chem.* **2013**, *5*, 342−347. (b) Nielsen, M.; Alberico, E.; Baumann, W.; Drexler, H.-J.; Junge, H.; Gladiali, S.; Beller, M. *Nature* **2013**, *495*, 85−89. (c) Alberico, E.; Sponholz, P.; Cordes, C.; Nielsen, M.; Drexler, H.-J.; Baumann, W.; Junge, H.; Beller, M. *Angew. Chem., Int. Ed.* **2013**, *52*, 14162−14166. (d) Hu, P.; Diskin-Posner, Y.; Ben-David, Y.; Milstein, D. *ACS Catal.* **2014**, 2649−2652. (e) Monney, A.; Barsch, E.; Sponholz, P.; Junge, H.; Ludwig, R.; Beller, M. *Chem. Commun.* **2014**, *50*, 707−709. (f) Campos, J.; Sharninghausen, L. S.; Manas, M. G.; Crabtree, R. H. *Inorg. Chem.* **2015**, in press, DOI: 10.1021/ic502521c.

(9) Koehne, I.; Schmeier, T. J.; Bielinski, E. A.; Pan, C. J.; Lagaditis, P. O.; Bernskoetter, W. H.; Takase, M. K.; Würtele, C.; Hazari, N.; Schneider, S. *Inorg. Chem.* **2014**, *53*, 2133−2143.

(10) (a) Chakraborty, S.; Dai, H.; Bhattacharya, P.; Fairweather, N. T.; Gibson, M. S.; Krause, J. A.; Guan, H. *J. Am. Chem. Soc.* **2014**, *136*, 7869−7872. (b) Chakraborty, S.; Brennessel, W. W.; Jones, W. D. *J. Am. Chem. Soc.* **2014**, *136*, 8564−8567. (c) Bornschein, C.; Werkmeister, S.; Wendt, B.; Jiao, H.; Alberico, E.; Baumann, W.; Junge, H.; Junge, K.; Beller, M. *Nat. Commun.* **2014**, *5*, 4111. (d) Bielinski, E. A.; Lagaditis, P. O.; Zhang, Y.; Mercado, B. Q.; Würtele, C.; Bernskoetter, W. H.; Hazari, N.; Schneider, S. *J. Am. Chem. Soc.* **2014**, *136*, 10234−10237. (e) Chakraborty, S.; Lagaditis, P. O.; Förster, M.; Bielinski, E. A.; Hazari, N.; Holthausen, M. C.; Jones, W. D.; Schneider, S. *ACS Catal.* **2014**, *4*, 3994−4003.

(11) (a) Smith, T. A.; Aplin, R. P.; Maitlis, P. M. *J. Organomet. Chem.* **1985**, *291*, c13−c14. (b) Yang, L.-C.; Ishida, T.; Yamakawa, T.; Shinoda, S. *J. Mol. Catal. A: Chem.* **1996**, *108*, 87−93. (c) Yamakawa, T.; Hiroi, M.; Shinoda, S. *J. Chem. Soc., Dalton Trans.* **1994**, 2265−2269. (d) Shinoda, S.; Yamakawa, T. *J. Chem. Soc., Chem. Commun.* **1990**, 1511−1512.

(12) Qu, S.; Dai, H.; Dang, Y.; Song, C.; Wang, Z.-X.; Guan, H. *ACS Catal.* **2014**, 4377−4388.

(13) In the experiment using a low catalyst loading of **2a** (0.001 mol %) it was possible to reduce the amount of $LiBF_4$ from 10 to 1 mol % with no decrease in catalytic activity.

(14) Zweifel, T.; Naubron, J.-V.; Büttner, T.; Ott, T.; Grützmacher, H. *Angew. Chem., Int. Ed.* **2008**, *47*, 3245−3249.

(15) Yang, X. *ACS Catal.* **2013**, *3*, 2684−2688.

(16) For a more detailed discussion of the differences between Yang's proposed pathway and our pathway see ref 10e.

(17) Azofra, L. M.; Alkorta, I.; Elguero, J.; Toro-Labbé, A. *J. Phys. Chem. A* **2012**, *116*, 8250−8259.

(18) Even though the best catalytic activity was observed using Li^+ as the LA, we computationally modeled the LA as Na^+. This is due to the difficulties in modelling the aggregation of Li^+, which can lead to the presence of clusters in solution.

(19) The decarboxylation of **D1** to form **D3** is thermodynamically disfavored. This indicates that CO_2 insertion into **D3** is thermody-

DOI: 10.1021/acscatal.5b00137
ACS Catal. 2015, 5, 2404−2415

namically favored and that these complexes may act as catalysts for CO_2 hydrogenation to formate. This is a topic of ongoing investigation in our laboratories.

(20) Yakelis, N. A.; Bergman, R. G. *Organometallics* **2005**, *24*, 3579−3581.

(21) Frisch, M. J.; Trucks, G. W.; Schlegel, H. B.; Scuseria, G. E.; Robb, M. A.; Cheeseman, J. R.; Scalmani, G.; Barone, V.; Mennucci, B.; Petersson, G. A.; Nakatsuji, H.; Caricato, M.; Li, X.; Hratchian, H. P.; Izmaylov, A. F.; Bloino, J.; Zheng, G.; Sonnenberg, J. L.; Hada, M.; Ehara, M.; Toyota, K.; Fukuda, R.; Hasegawa, J.; Ishida, M.; Nakajima, T.; Honda, Y.; Kitao, O.; Nakai, H.; Vreven, T.; Montgomery, J. A., Jr.; Peralta, J. E.; Ogliaro, F.; Bearpark, M.; Heyd, J. J.; Brothers, E.; Kudin, K. N.; Staroverov, V. N.; Kobayashi, R.; Normand, J.; Raghavachari, K.; Rendell, A.; Burant, J. C.; Iyengar, S. S.; Tomasi, J.; Cossi, M.; Rega, N.; Millam, N. J.; Klene, M.; Knox, J. E.; Cross, J. B.; Bakken, V.; Adamo, C.; Jaramillo, J.; Gomperts, R.; Stratmann, R. E.; Yazyev, O.; Austin, A. J.; Cammi, R.; Pomelli, C.; Ochterski, J. W.; Martin, R. L.; Morokuma, K.; Zakrzewski, V. G.; Voth, G. A.; Salvador, P.; Dannenberg, J. J.; Dapprich, S.; Daniels, A. D.; Farkas, Ö.; Foresman, J. B.; Ortiz, J. V.; Cioslowski, J.; Fox, D. J. *Gaussian 09*, revision D.02; Gaussian, Inc.: Wallingford, CT, USA, 2009.

(22) (a) Lee, C.; Parr, R. G.; Yang, W. *Phys. Rev. B* **1988**, *37*, 785−789. (b) Becke, A. D. *Phys. Rev. A: At., Mol., Opt. Phys.* **1988**, *38*, 3098−3100. (c) Becke, A. D. *J. Chem. Phys.* **1993**, *98*, 5648−5652.

(23) Weigend, F.; Ahlrichs, R. *Phys. Chem. Chem. Phys.* **2005**, *7*, 3297−3305.

DOI: 10.1021/acscatal.5b00137
ACS Catal. 2015, 5, 2404−2415